Materials Science & Engineering C 90 (2018) 159–167

Contents lists available at ScienceDirect

Materials Science & Engineering C

journal homepage: www.elsevier.com/locate/msec

Bone marrow-derived mesenchymal stem cells laden novel thermo-sensitive hydrogel for the management of severe skin wound healing

Zhang Lei[a,1], Gurankit Singh[b,1], Zhang Min[a], Chen Shixuan[a], Kaige Xu[b], Xu Pengcheng[a], Wang Xueer[a], Chen Yinghua[a], Zhang Lu[a,c,*], Zhang Lin[a,**]

[a] Guangdong Provincial Key Laboratory of Construction and Detection in Tissue Engineering, Guangdong Provincial Key Laboratory of Proteomics and Key Laboratory of Transcriptomics and Proteomics of Ministry of Education of China, School of Basic Medical Sciences, Southern Medical University, Guangzhou, 510515, China
[b] Department of Mechanical Engineering, Biochemistry and Medical Genetics, University of Manitoba, Manitoba Institute of Child Health, Winnipeg, MB R3T 2N2, Canada
[c] Elderly Health Services Research Center, Southern Medical University, Guangzhou 510515, China

ARTICLE INFO

Keywords:
Skin wound healing
Hydrogel
Bone marrow-derived mesenchymal stem cells (BMSCs)
Fibroblast growth factor (FGF)
Transforming growth factor beta 1 (TGF-β1)

ABSTRACT

Bone marrow-derived mesenchymal stem cells (BMSCs) are easy to collect and culture, and it is identified that it has multi-directional differentiation potential, moreover it has low immunogenicity, hence it can be used as an allogeneic cell source for skin wound healing. Hydrogel has been widely used in skin wound healing own to it is able to mimic the 3D microenvironment of cells, which supports cell proliferation, migration and secretion. In this study, we created a novel biocompatible thermo-sensitive hydrogel to carry BMSCs for full-thickness skin wound healing. The thermo-sensitive hydrogel loaded with BMSCs can fast achieve sol-gel transition after implanting to the wound. Histological results confirmed that hydrogel-BMSCs combination group showed significant promotion of wound closure, epithelial cells' proliferation and re-epithelialization, and reduced inflammatory responses in the wounds and in the tissues surrounding the wounds. The combination therapy also can promote collagen deposition, TGF-β1 and bFGF secretion and tissue remodeling. The present study provides a promising strategy for the clinical treatment of skin wounds.

1. Introduction

Skin is the largest organ of the human body and is the first barrier to the external environment. Skin wound healing is a common problem and a major challenge for large-area trauma, burn and no healing diabetic skin wound [1]. In recent years, the effects of stem cell transplantation on skin wound healing have been extensively studied [2,3]. Researchers have proven that bone marrow stromal cells (BMSCs) have a positive effect on promoting wound healing. The current researches showed that BMSCs used as seed cells for transplantation, it can secrete various types of cytokines and growth factors, such as transforming growth factor beta 1 (TGF-β1) and basic fibroblast growth factor (bFGF), which can promote the formation of granulation tissue in wounds, assist in the regeneration of skin appendages after epithelization [4–6]. BMSCs can also differentiate into vascular endothelial cells, epidermal cells and other skin appendage structures to participate in wound repair [7–11].

Absorbent cotton medical gauze is primarily used as a conventional dressing for clinical applications. Despite its wide use, gauze has a number of disadvantages. For example, its absorbency is not sufficiently high, it needs to be frequently changed, it is prone to adhere to wounds, and it can lead to secondary trauma. Biological dressings mainly include freeze-dried pork skin and amniotic membranes, although they have significant advantages over conventional absorbent cotton medical gauze, biological dressings still have insurmountable disadvantages, including their limited application, the risk of spreading bacterial, fungal and viral diseases, and the possibility of immunological rejection [12–15].

As an alternative, thermo-sensitive hydrogels can prevent the loss of water and body fluid from wounds, additionally, thermo-sensitive hydrogels can not only adhere to irregularly surfaced wounds but can also resist the invasion of bacteria. Due to their good water-absorption capacity and degradability, thermo-sensitive hydrogels can avoid secondary trauma during the dressing change [16–19]. Furthermore, thermo-sensitive hydrogels provide a temporary support substratum for cell transplantation, as the porous internal structure of thermo-sensitive hydrogels provides a suitable space for cell proliferation and differentiation and for nutrient exchange [20–23].

* Correspondence to: Z. Lu, Elderly Health Services Research Center, Southern Medical University, Guangzhou 510515, China.
** Corresponding author.
E-mail addresses: zlulu70@126.com (Z. Lu), zlilyzh@126.com (Z. Lin).
[1] These authors contributed equally to this work.

https://doi.org/10.1016/j.msec.2018.04.045
Received 30 November 2017; Received in revised form 30 March 2018; Accepted 16 April 2018
Available online 17 April 2018
0928-4931/

Herein, in the present study, a thermosensitive hydrogel that was developed in our group and explored the therapeutic effects of this thermo-sensitive hydrogel encapsulated with BMSCs for the treatment of a full-thickness wound in a mouse model.

2. Materials and methods

2.1. Materials

N, N′-bis (acryloyl) cystamine, N-Isopropylacrylamide (NIPAM), Agmatine sulfate salt (AS), 1-(2-Aminoethyl)-piperozine (AEPZ), *N*,*N*,*N*′,*N*′-Tetramethylethanediamine (TEMED), Ammonium persulfate (APS), Lithium hydroxide (LiOH) and dithiothreitol (DTT), all the chemicals were purchased from Sigma-Aldrich. Bromodeoxyuridine (BrdU) (Sigma), α-smooth muscle actin (α-SMA) (Boster), keratin 1 (K1) (Abcam) and keratin 6 (K6) (Covance). CCK-8 proliferation assay kit was purchased from Fisher Scientific. DMEM medium, fetal bovine serum (FBS). glutamine and penicillin-streptomycin were ordered from Invitrogen. Cell culture plate was ordered from Corning. The basic-FGF and TGF-β1 ELISA kit were purchased from Shanghai Licheng Biological Technology co., LTD, China.

2.2. Synthesis of hyperbranched PAA crosslinker

MBA (234 mg, 1.52 mmol), Agmatine (138 mg, 0.6 mmol) and AEPZ (52 mg, 0.4 mmol) were dissolved in water/methanol (*v*/v = 5/1, total in 5 ml) while stirring. When the solution was clear, LiOH·H2O (25.2 mg, 0.6 mmol) was added to the solution. The mixture was then gently stirred and allowed to react at 40 °C in the dark for 72 h. After the reaction, the solvent was evaporated using a rotary-evaporator. The product was finally recovered by lyophilization and stored in-20 °C refrigerator for future use.

2.3. Characterization of hyperbranched PAA crosslinker

The hyperbranched PAA crosslinker was characterized by fourier transforms infrared spectroscopy (FTIR) and ^{1}H NMR, the detailed information as following. FTIR spectra were recorded with a Thermo Scientific IR100 FT-IR Spectrometer. PAA crosslinkers were freeze-dried in order to remove the residual chemicals. Then dried PAA crosslinkers were ground to powder, mixed with KBr, and compressed into pellets, then FTIR spectra were performed. In order to further characterize the hyperbranched PAA crosslinker, 1H NMR spectra (Fig. 1B) was recorded on an Advance 300 MHz spectrometer (Bruker). 8 mg of PAA crosslinker powders were dissolved in 800 μl of D2O. 1H NMR (ppm): *δ*, 1.5 (-N-CH2-CH2-CH2-CH2-NH-,s, 4 mH), 2.0–3.0(CO-CH2-CH2-N,m, 8(m + 2)H, -N2C4H8-CH2-CH2-N-,m, 8nH), 3.17(-N-CH2-CH2-,s, 2 mH), 4.53 and 4.62(-NH-CH2-CH-,s, 2 m + 2H), 5.77 (CH2 = CH-,t, 2H), 6.21(CH2 = CH-,s, 2H), 6.225 (-CH2 = CH,s, 2H).

2.4. Fabrication of thermo-sensitive hydrogel with hyperbranched PAA crosslinker

PAA crosslinked poly-NIPAM hydrogels were prepared at the concentration of 60 mg/ml with the ratio NIPAM: PAA = 5:1. Gels were fabricated in distill water by initiator APS (5.7 mg/ml) and catalyst TEMED (2.9 mg/ml) at room temperature for 30 min.

2.5. Characterization of physical properties

2.5.1. Swelling behavior test

The hydrogel was fabricated into a 2-mm-thick cylinder with a diameter of 10 mm and was then freeze-dried. The dry weight of this cylinder, W_0, was then measured. The dried cylinder was then placed in phosphate-buffered saline (PBS) (0.01 M; pH 7.4) at 37 °C and allowed to swell for 1.5 h, 3 h, 6 h, 9 h, 12 h or 24 h. The wet weight of the cylinder, Wt, was measured at each time point. The swelling ratios were calculated using equation (Eq.) [1]. For this test, $n = 6$, and the measurement was repeated 3 times [24].

$$\text{Swelling ratio (\%)} = (Wt - Wo)/Wo \times 100\% \quad (1)$$

2.5.2. In vitro degradation performance test

The hydrogel was fabricated into a 2-mm-thick cylinder with a diameter of 10 mm. After it was freeze-dried, the hydrogel cylinder was evenly divided into 4 parts. The dry weight of each of the 4 parts, Wd, was measured. Each of the 4 parts was then separately immersed into PBS (0.01 M; pH 7.4) containing 1 mol/ml DTT at 37 °C. The 4 parts were then harvested, one each on the 8, 16, 24 and 32 days. The remainder of each harvested part was first rinsed 3 times with distilled water at 37 °C and was then freeze-dried, after which the weight of the remaining part of hydrogel cylinder, Ww, was determined. The degradation rates were calculated using Eq. (2) [25]. For this test, $n = 6$, and the measurement was repeated 3 times.

$$\text{Degradation rate (\%)} = (Wd - Ww)/Wd \times 100\% \quad (2)$$

2.5.3. Hydrogel toxicity analysis

In accordance with International Organization for Standardization (ISO) 10993-5, extracts were prepared using 1 ml of Dulbecco's modified Eagle's medium (DMEM, Invitrogen, Carlsbad, CA) for every 0.75 cm^2 of hydrogel. The hydrogel was laid flat in a 6-cm petri dish and UV sterilized for 30 min. DMEM was then added to the proportions described above, and the hydrogel was placed in a 37 °C incubator for 5 days for extraction. The hydrogels and extracts were then collected into 50 ml centrifuge tubes and centrifuged at 7000 rpm for 10 min. The supernatant was collected and filter sterilized as 100% hydrogel extracts. DMEM was used to dilute the 100% extracts to prepare 50% extracts. The toxicity of the hydrogel was evaluated using the CCK-8 proliferation assay kit [26]. First, one hundred milliliter L929 fibroblasts suspension (5×10^3 cells) were seeded in each well of 96-well plate and cultured for 24 h, after which the culture medium was removed. The 50% and 100% hydrogel extraction media were then added to the wells respectively. After the fibroblasts were cultured in different conditioned media for 1 day, 2 days or 3 days, 10 μL of CCK-8 was added into each well, and the fibroblasts were further incubated for 3 h. The absorption values at 450 nm were determined using an enzyme mark instrument (BIO-RAD). The relative proliferation rates were calculated using Eq. (3). There were 6 replicate wells in each group, and each measurement was repeated 3 times.

$$\text{Relative proliferation rate (\%)} = (\text{the sample})/(\text{the negative control}) \times 100\% \quad (3)$$

2.6. Culture and encapsulation of BMSCs

One healthy 8- to 12-week-old male C57BL/6 mice were purchased from the Laboratory Animal Centre of Southern Medical University. Briefly, bone marrow was obtained as in our previous study and then centrifuged at 1500 rpm for 5 min. The supernatant was discarded, and the precipitate was re-suspended in DMEM medium plus with 10% FBS. 1% glutamine and 1%penicillin-streptomycin, transferred into a petri dish, and cultured in an incubator at 37 °C and 5% CO2. The medium was replaced every 2 days, as the cells were subcultured once cell fusion reached 90% [27].

Fourth-generation BMSCs were trypsinized in 0.25% trypsin and centrifuged. Afterwards, the BMSCs were resuspended in saline and counted (cell concentration: 1 × 106 cells/ml). The BMSCs were again centrifuged, and 100 μl hydrogel was added to the centrifuged BMSCs. The hydrogel and the BMSCs were mixed to homogeneity using a pipette tip [28].

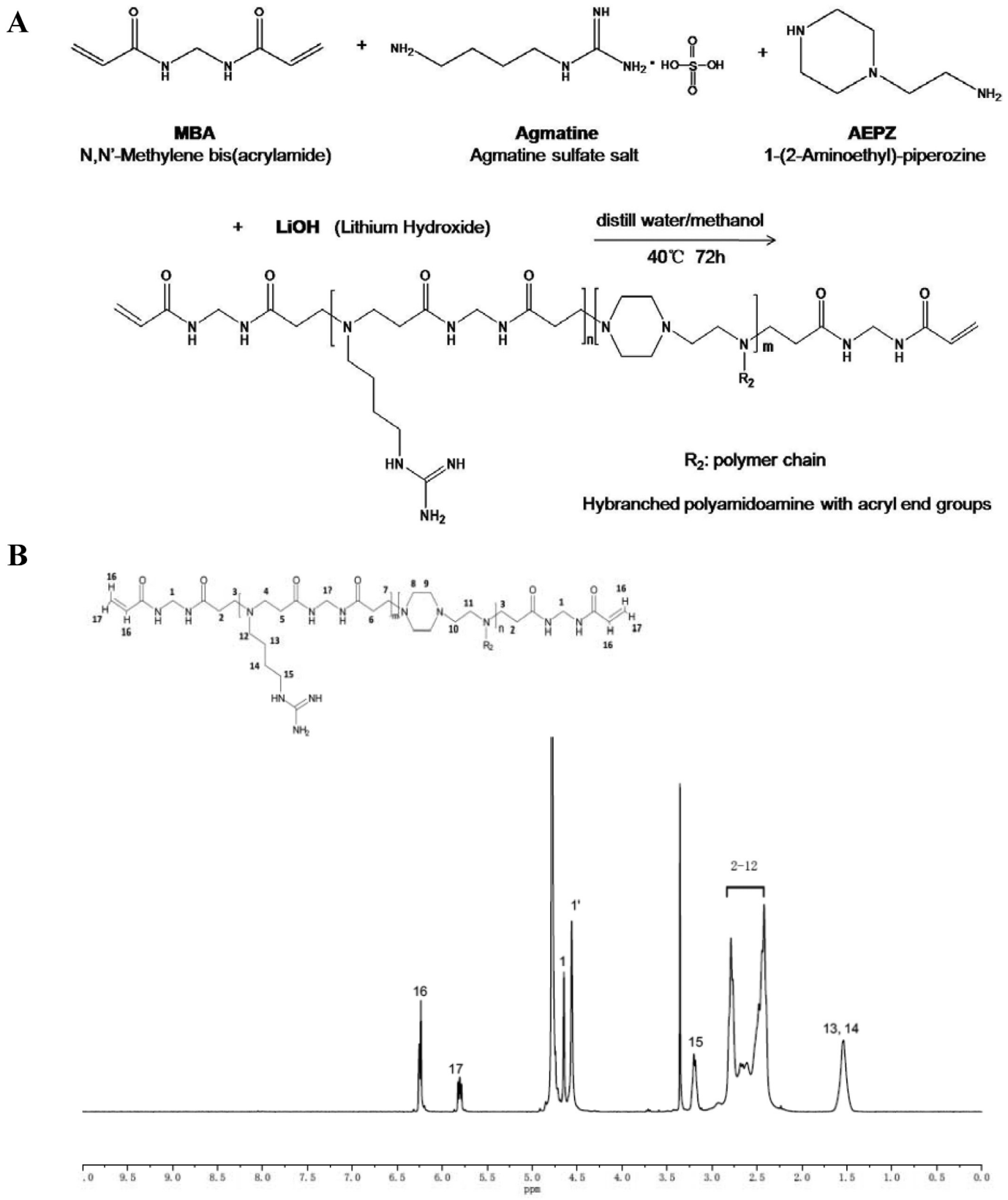

Fig. 1. The preparation of hyperbranched PAA crosslinker. (A)Schematic illustration of the preparation of hyperbranched PAA crosslinker. (B) ^{1}H NMR spectrum of the PAA crosslinker.

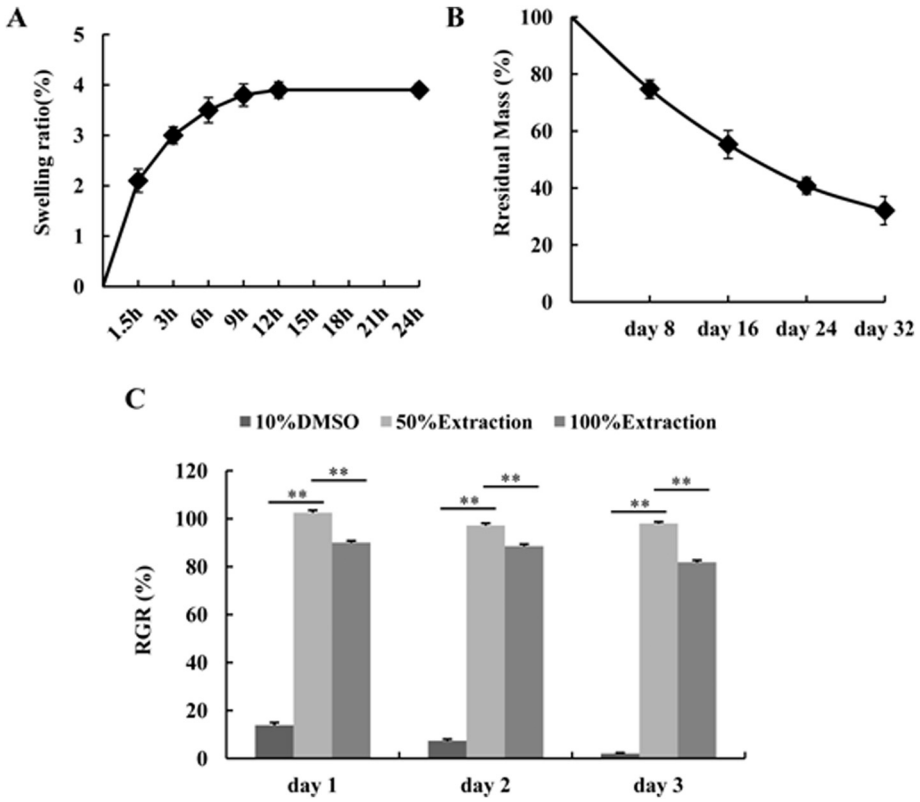

Fig. 2. Characterization of the physical properties and toxicity analysis of the hydrogel. (A) Swelling ratios of the hydrogel at 1.5 h, 3 h, 6 h, 9 h, 12 h and 24 h respectively. (B) Remaining mass percentage of the hydrogel on the 8th, 16th, 24th and 32nd days respectively.(C) Relative proliferation rates of L929 cells after culture in 50% and 100% hydrogel extraction media or in a complete medium that contained 10% DMSO for 1 day, 2 days and 3 days respectively.

2.7. Wound model

Twenty-four healthy adult specific-pathogen-free (SPF)-class C57 mice were randomized into 4 groups: a control group, a BMSCs-alone group, a hydrogel-alone group and a hydrogel-BMSCs combination group. The mice were anesthetized by intraperitoneal injection of 10% chloral hydrate (0.003 ml/g). After the hairs on one side of the back of each C57 mouse were shaved, the remaining hairs were removed using frozen honey wax. Next, a square-shaped (1-cm2) incision that was deep enough to penetrate the subcutaneous tissue was created [29]. After the operation, the mice had free access to food and water. The healing of the wounds on each mouse was recorded using a digital camera on the day of the operation and again on the 3, 5, 7 and 14 days after the operation. The wound-healing rates were calculated using the following equation: wound-healing rate = (the area of the original wound − the area of the unhealed wound) / the area of the original wound × 100%. The Bioethics Committee of Southern Medical University approved all animal experiments, which were in accordance with the National Institutes of Health (NIH) Guide for the Care and Use of Laboratory Animals.

2.8. Histological observations

After 3, 5, 7, 14 days treatment, the wound and surrounding tissue (0.5 cm) were carefully excised, rinsed in PBS, and then fixed in 4% Paraformaldehyde (PFA). Samples were dehydrated in a graded ethanol series (70–100%) and embedded in paraffin. Five-micrometer sections were prepared. According to the standard procedures, samples were stained with either hematoxylin and eosin (HE) or masson trichrome, and immunohistochemistry including F4/80 (eBioscience), bromodeoxyuridine (BrdU) (Sigma), α-smooth muscle actin (α-SMA) (Boster), keratin 1 (K1) (Abcam) and keratin 6 (K6) (Covance).

Image-Pro Plus was used to analyze the average optical density values for K1, K6, α -SMA expression. Five randomly selected fields of view were examined for each group at each time point and used to assess the average optical density value per unit area. Statistics regarding the number of positively stained cells for BrdU were obtained using five randomly selected fields of view for each group at each time point.

2.9. Enzyme-linked immunosorbent assay (ELISA)

A piece of skin located 0.5 cm from the wound of each mouse was excised on the 3, 5, 7 and 14 days after the operation. The skin was rinsed with saline and weighed. Next, the skin was homogenized at 4 °C with an amount of saline equal to 10 times the weight of the skin. The homogenate was then centrifuged at 3000 rpm for 20 min, and the supernatants were stored in liquid nitrogen. An appropriate plate was taken from the ELISA kit, and blank wells, standard wells and sample wells for the assay were set. Horseradish peroxidase was added to the standard wells and the sample wells, and the plate was incubated at 37 °C for 60 min. After the plate was washed, 50 μL of substrate A and 50 μL of substrate B were added to all of the wells, and the plate was then incubated for 15 min before a terminating reagent was added. The OD of each well was measured at 450 nm [30].

2.10. Statistical analysis

Statistical analysis was performed using Statistical Package for the Social Sciences (SPSS) 13.0 software (IBM). All the data are expressed in the form of mean value ± standard deviation. Differences among the groups were assessed using one-way ANOVA. A value of $p < 0.05$ was considered statistically significant (significance levels: *p < 0.05 and **$p < 0.01$).

3. Results and discussion

3.1. Synthesis and characterization of hyperbranched PAA crosslinker

The agmatine and AEPZ contained hyperbranched poly

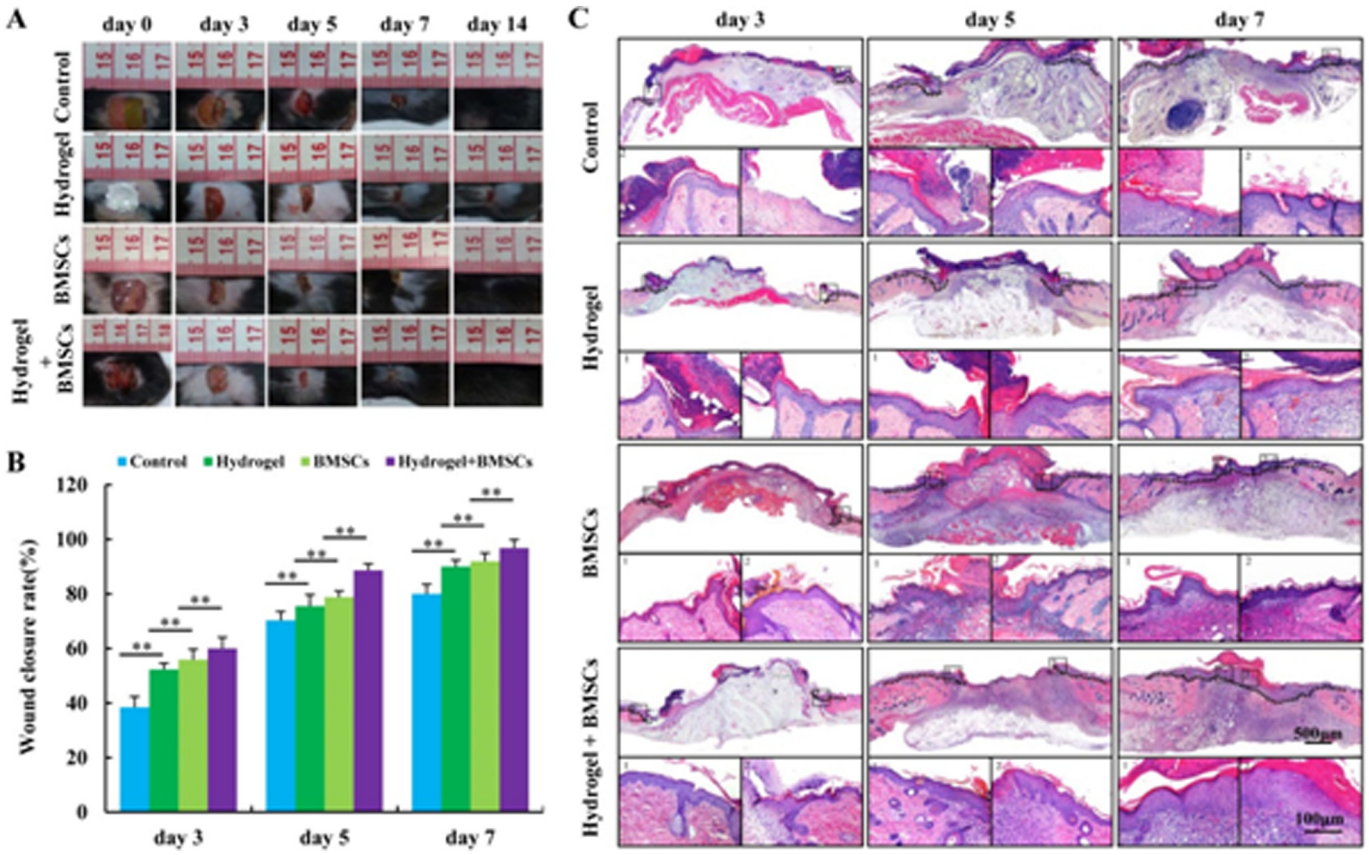

Fig. 3. Hydrogel combined with BMSCs promoted wound healing. (A) General wound-healing conditions of the mice in the control group, the hydrogel group, the BMSCs group and the hydrogel–BMSCs combination group 3 days, 5 days, 7 days and 14 days after the operation. (B) Comparison of the wound-healing rates of mice in the control group, the hydrogel group, the BMSCs group and the hydrogel–BMSCs combination group 3 days, 5 days and 7 days after the operation. (C) H&E staining of the wounds of the mice in the control group, the hydrogel group, the BMSCs group and the hydrogel–BMSCs combination group 3 days, 5 days and 7 days after the operation. *$p < 0.05$, **$p < 0.01$.

(amidoamine) (PAA) crosslinker was synthesized via Michael-addition polymerization as shown in Fig. 1A. Fig. S1 showed the FTIR spectra of hyperbranched crosslinker, the sharp peaks appeared around 1650.66 cm-1 was attributed to the C═O stretching frequency from MBA. While peaks located at 1533.51 cm-1 was attributed to the NH2 group from agmatine and AEPZ, the results show successful conjugation of hyperbranched PAA crosslinker. In order to further determine the chemical structure of hyperbranched PAA crosslinker, we sued ^{1}H NMR to confirm it. As shown in Fig. 1B, the 1H NMR results further verified the PAA crosslinker structure was the same as desired.

3.2. Synthesis and characterization of the thermo-sensitive hydrogel

The NIPAM and PAA were fabricated via radical polymerization due to the vinyl groups from the PAA crosslinker [31,32]. As shown in Fig. S2, the hydrogel was transparent and soft, more like liquid at room temperature, when it was heated to 37 oC, the hydrogel became white and solid. It suggested that the hydrogel is thermo-sensitive. Following we explored the swelling behavior and degradation behavior of the hydrogel. The swelling behavior of hydrogel was tested to evaluate the maximum liquid-absorption capacity. As shown in Fig. 2A, the swelling ratio of the hydrogel approached its maximal value at 12 h, the value is (3.9 ± 0.16)%. The degradation behavior of hydrogel in DTT solution, because the DTT solution can mimic the residual environment of the human body. As shown in Fig. 2B, The hydrogel can be gradually degraded, it is biodegradable (Fig. 2B). Fig. 3C showed the relative proliferation rates of L929 cells in media extracted from the hydrogel. According to the ISO 10993-5 standard, the 50% and 100% extraction media of the hydrogel had a Class 1 toxicity level, whereas the positive control group showed a Class 4 toxicity level. These results show that the thermo-sensitive hydrogel exhibited a relatively high level of biological safety, it mainly own to the induction of agmatine, which is similar to the RGD peptides that modified the PNIPAM hydrogel to enhance cell adhesion and proliferation [33].

3.3. Hydrogel-BMSCs combination therapy promotes wound closure

After wound occurred, the primary task is let the wound quickly close [34]. So we observed the post-operational wound-healing times and statistically analyzed the wound closure rates with different treatments. We found that five and seven days after transplantation, the wound-healing rates of hydrogel-BMSCs combination group were significantly higher than those of the mice in the hydrogel-alone group ($p < 0.01$), the BMSCs group or the control group ($p < 0.01$) (Fig. 3A and Fig. 3B). Furthermore, the wounds of the mice in the hydrogel-BMSCs combination group closed earlier than those of the mice in the hydrogel-alone group, the BMSCs group or the control group. The histological results showed the re-epithelialization of the hydrogel-BMSCs combination group were higher than those of the mice in the hydrogel-alone group, the BMSCs group or the control group on the 3, 5 and 7 days respectively (Fig. 3C). These results show that the combination of hydrogel with BMSCs could promote wound closure.

3.4. Hydrogel-BMSCs combination therapy promote myofibroblasts formation

The wound contraction force is derived from myofibroblast, which highly expresses α-SMA [35]. So we used immunohistochemistry

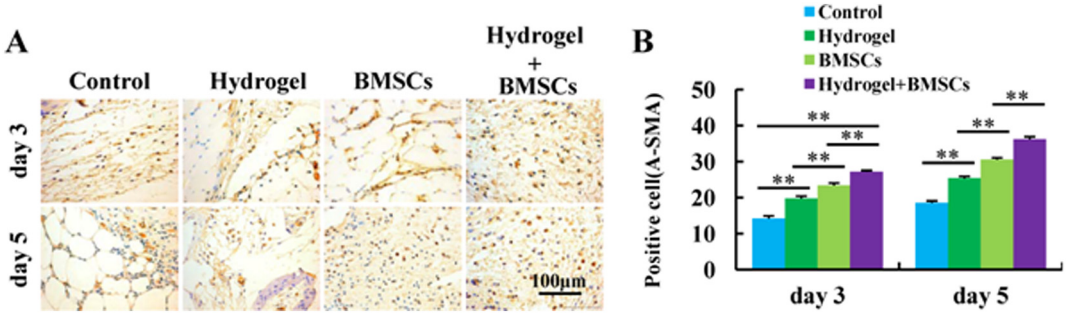

Fig. 4. Hydrogel combined with BMSCs promotes the contraction of wounds and reduces inflammatory responses at wound sites. (A) Expression of α-SMA in the wounds of the mice in the control group, the hydrogel group, the BMSCs group and the hydrogel-BMSCs combination group 3 and 5 days after the operation, as revealed by immunohistochemical examination. (B) Statistical results for the numbers of α-SMA-positive cells at the wound sites of mice in the control group, the hydrogel group, the BMSCs group and the hydrogel-BMSCscombination group. Scale bar: 100 μm. *p < 0.05, **p < 0.01.

technology to detect the expression of α-SMA in the four groups. As shown in Fig. 4, three and five days after the trauma, the expression of α-SMA in the wounds of the mice in the hydrogel-BMSCs combination group was significantly higher than the other three groups ($p < 0.01$). This result could clearly explain that the wound closure rate was the fastest in the hydrogel-BMSCs combination group.

3.5. Hydrogel-BMSCs combination therapy promote skin cells proliferation

Keratinocytes and fibroblasts are the two major cells of the skin after wound occurred, keratinocytes and fibroblasts proliferate first, then migrate to the wound area [36]. Hence we used BrdU and Keratin 6 to detect the proliferation of fibroblast and keratinocytes respectively. As shown in Fig. 5A and Fig. 5B, the BrdU positive cells in the hydrogel-BMSCs combination group were significantly higher than the other three groups ($p < 0.01$) at each detected time point. When the keratinocytes proliferate, they strongly express K6. As shown in Fig. 5C and Fig. 5D, the expression of K6 in the hydrogel-BMSCs combination group was also evidently higher than the other three groups ($p < 0.01$). These results revealed that hydrogel-BMSCs combination therapy promotes fibroblast proliferation in dermis and keratinocytes proliferation in the epidermis, which lay the foundation for wound tissue regeneration.

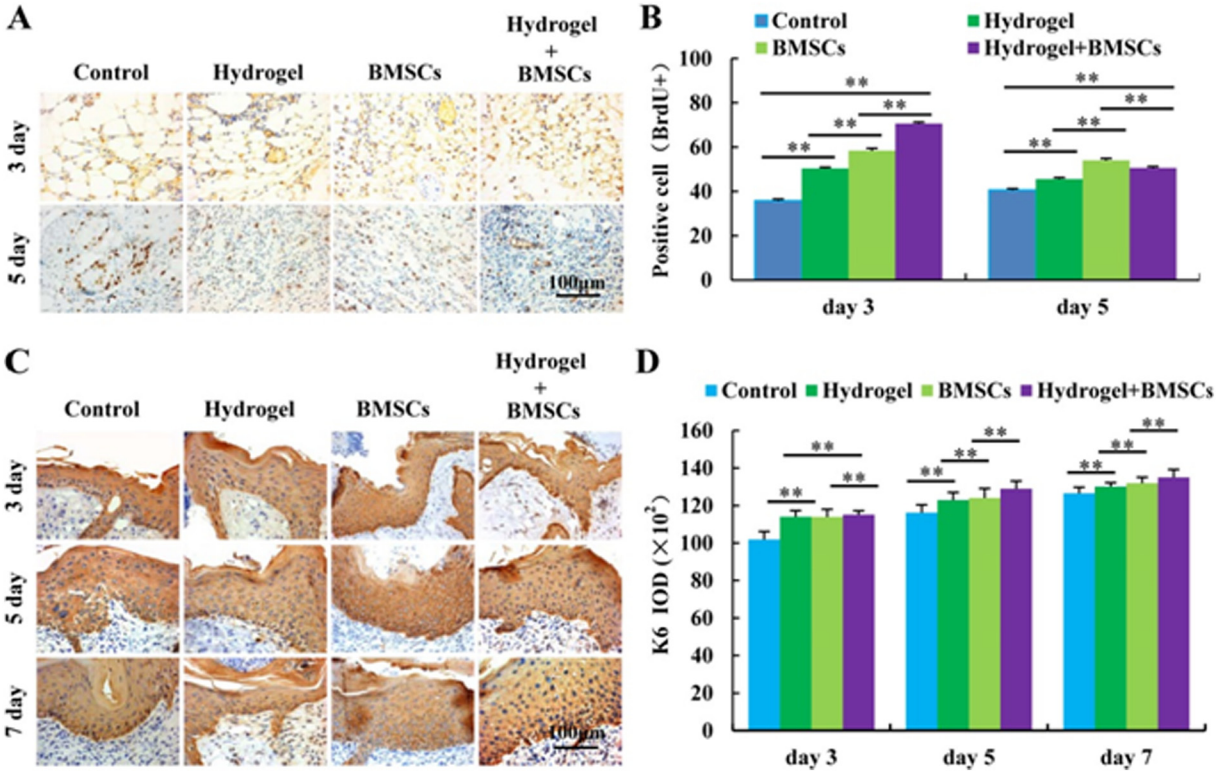

Fig. 5. The hydrogel-BMSCs combination promotes the proliferation of cells in wounds and around wound edges. (A) BrdU staining in and around the wounds of mice in the control group, the hydrogel group, the BMSCs group and the hydrogel-BMSCs combination group 3 and 5 days after the operation, as revealed by immunohistochemical examination. (B) Statistical results for BrdU staining in and around the wounds of mice in the control group, the hydrogel group, the BMSCs group and the hydrogel-BMSCs combination group. (C) Expression of K6 at the wound sites of mice in the control group, the hydrogel group, the BMSCs group and the hydrogel-BMSCs combination group 3, 5 and 7 days after the operation, as revealed by immunohistochemical examination. (D) Statistical results of the expression of K6 at the wound sites of mice in the control group, the hydrogel group, the BMSCs group and the hydrogel-BMSCs combination group. Scale bar: 100 μm. **p < 0.01.

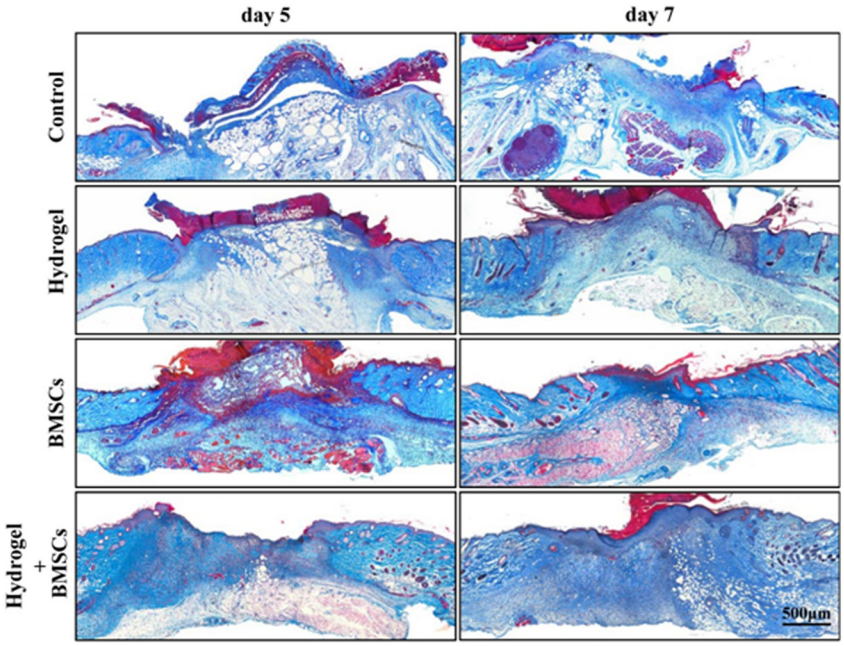

Fig. 6. The hydrogel-BMSCs combination promotes the synthesis of collagen in wounds. The synthesis and deposition of newly formed collagen in the wounds of the control group, the hydrogel group, the BMSCs group and the hydrogel-BMSCs combination group 5 and 7 days after the operation were examined using Masson's trichrome staining method. Scale bar: 500 μm.

3.6. Hydrogel-BMSCs combination therapy promote collagen deposition

We have demonstrated that hydrogel-BMSCs combination therapy promote fibroblast proliferation in dermis, meanwhile, the proliferated fibroblast will start to secrete ECM, and collagen is the major ECM [37]. Collagen deposition plays an important role in the wound repair process, it can provide a structural support for cell proliferation, migration, and differentiation [38]. As shown in Fig. 6, five days and 7 days after trauma, the amounts of newly formed collagen in the hydrogel-BMSCs combination group were more than the other three groups. And there was no significant difference between the hydrogel-alone group and the BMSCs group in the amount of newly formed collagen. These results suggested the hydrogel-BMSCs combination therapy was able to promote collagen deposition.

3.7. Hydrogel-BMSCs combination therapy promote FGF and TGF-β1 secretion

Extensive researches have shown that growth factors play important roles during the skin wound healing process, they can regulate cell proliferation, differentiation, migration, and secretion [39,40]. For example, TGF-β1 can stimulate fibroblasts to synthesize large amounts of type I, type II, type III and type IV collagen, which provide a temporary ECM for the ingrowth of capillaries and the migration of basal cells [41]. In addition, TGF-β1 can promote fibroblasts to transform into myofibroblasts, which can highly express α-SMA and make wound contraction [42,43]. Another key growth factor in the wound healing is basic fibroblast growth factor (bFGF). bFGF not only can promote wound healing but also can help tissue remodeling after wound closure, it is related to the downregulating type-I procollagen gene expression, which counteracts the excessive deposition of collagen by keloid fibroblasts and prevents keloid formation [44,45].

Hence, the expression levels of TGF-β1 and bFGF were analyzed using ELISA. As shown in Fig. 7A, the levels of TGF-β1 in the wound tissues showed an increasing trend 3 and 5 days after the operation, while they started decreasing on the 7 days after the operation. After trauma, the levels of TGF-β1 in the hydrogel-BMSCs combination group were significantly higher than the other three groups on both 3 days and 5 days ($p < 0.01$). Seven days after trauma, the levels of TGF-β1 in the hydrogel-BMSCs combination group, the hydrogel-alone group, and the BMSCs group had decreased to some extent, whereas the levels of TGF-β1 in the control group still exhibited an increasing trend. Additionally, the levels of TGF-β1 in the hydrogel-BMSCs combination group were lower than in the hydrogel-alone group ($p < 0.01$) or the BMSCs group ($p < 0.01$), there was no significant difference between the TGF-β1 levels of the BMSCs group and the hydrogel-alone group ($p > 0.05$).

As shown in Fig. 7B, the levels of bFGF in all groups exhibited an

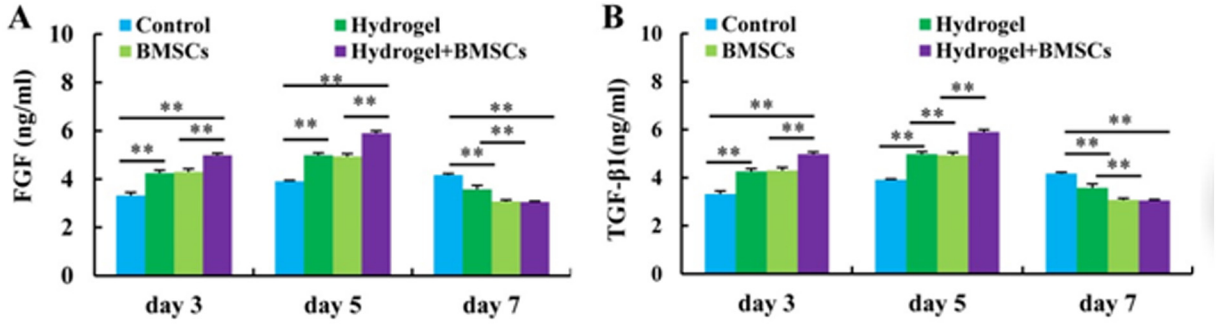

Fig. 7. The hydrogel-BMSCs combination promotes the expression of FGF and TGF-β1 at wound sites and regulates the reconstruction of wound tissues. (A) Quantitatively analyzed secreted FGF levels at the wound sites of mice in the control group, the hydrogel group, the BMSCs group and the hydrogel-BMSCs combination group 3, 5 and 7 days after the operation. (B) quantitatively analyzed secreted TGF-β1 levels at the wound sites of mice in the control group, the hydrogel group, the BMSCs group and the hydrogel-BMSCs combination group 3, 5 and 7 days after the operation.

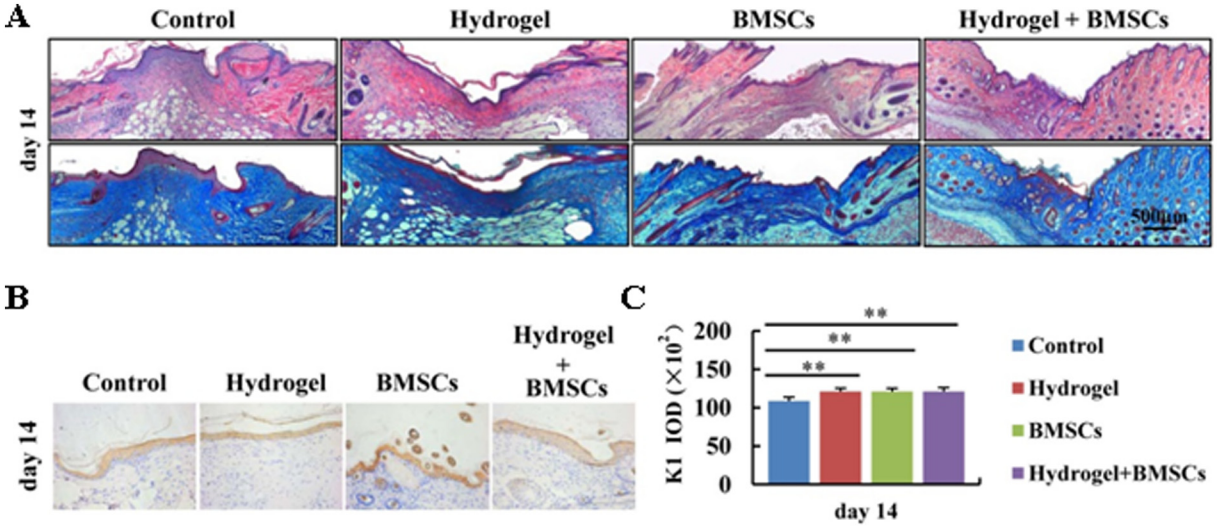

Fig. 8. (A) H&E and Masson staining of the wounds of mice in the control group, the hydrogel group, the BMSCs group and the hydrogel-BMSCs combination group 3, 5 and 7 days after the operation. (B) Expression of K1 at the wound sites of mice in the control group, the hydrogel group, the BMSCs group and the hydrogel-BMSCs combination group 14 days after the operation, as revealed by immunohistochemistry. (C) Statistical analysis of K1 expression at the wound sites of mice in the control group, the hydrogel group, the BMSCs group and the hydrogel-BMSCs combination group. Scale bar: 100 μm. **p < 0.01.

increasing trend in the first five days after trauma. Seven days after trauma, the levels of bFGF in the hydrogel-BMSCs combination group, the hydrogel-alone group, and the BMSCs group exhibited a decreasing trend. After trauma, the levels of bFGF in the hydrogel-BMSCs combination group were significantly higher than the other three groups on both 3 days and 5 days ($p < 0.01$). And there was no significant difference between the bFGF levels of the hydrogel-alone group and the BMSCs group ($p > 0.05$). In addition to the control group, the levels of bFGF in the other 3 groups exhibited a decreasing trend on the 7 days. The levels of bFGF in the hydrogel-BMSCs combination group were significantly lower than the hydrogel-alone group ($p < 0.01$) and control group ($p < 0.01$). And there was no significant difference between the levels of bFGF in the hydrogel-BMSCs combination group and the BMSCs group ($p > 0.05$).

3.8. Hydrogel-BMSCs combination therapy promote tissue remodeling after wound healing

After wound healing, the ECM needs to remodel, the exceed ECM will degrade until new formed ECM structure close to the normal tissue [31]. As shown in Fig. 8A, the masson staining also showed that the regenerated dermal tissue in the wounds of the mice in the hydrogel-BMSCs combination group was similar to the normal tissue, while the regenerated dermal tissue of other 3 groups were relatively dense, which suggested the tissue remodeling was not finished. Moreover, we also explored the epidermis maturation among the four groups. K1 is one of the markers for keratinocyte terminal differentiation. As shown in Fig. 8B and Fig. 8C, the expression of K1 in the control group lower than the other three groups ($p > 0.01$). There was no significant difference between the hydrogel-BMSCs combination group and the hydrogel-alone group ($p > 0.05$), however, was there a significant difference between the expression of K1 in the hydrogel-BMSCs combination group and the BMSCs group ($p > 0.05$). These results show that the hydrogel-BMSCs combination therapy had positive effects on promoting the keratinocytes maturation. These results revealed that hydrogel-BMSCs combination therapy promotes epidermis and dermis remodeling after wound healing.

4. Conclusions

In summary, we showed the therapeutic effect of a thermo-sensitive hydrogel in combination with BMSCs on skin wound healing. We discovered the hydrogel could provide a relatively aseptic and stable environment for the wounds and the transplanted BMSCs, and it had positive effects on the migration and proliferation of epithelial cells, the deposition of collagen, the secretion of growth factors and wound-healing quality. The hydrogel-BMSCs combination therapy exhibited a markedly therapeutic effect than the hydrogel or BMSCs alone. Our study has introduced a new concept for treating skin trauma and supporting clinical treatment. However this work has limitations, the mechanisms of BMSCs induced wound healing is not clear, the detailed signaling pathway need be explored in the future works.

Acknowledgement

This work was supported by the Natural Science Foundation of China (81371719, 81371509, 81472166, 81430045 and 81571860) and the Colleges Pearl River Scholar Funded Scheme (GDUPS2013, GDUPS2015). The project supported by Guangdong Natural Science Foundation (2014A030312013).

Appendix A. Supplementary data

Supplementary data to this article can be found online at https://doi.org/10.1016/j.msec.2018.04.045.

References

[1] M. Zhang, L. Sun, X. Wang, S. Chen, Q. Jia, N. Liu, Y. Chen, Y. Kong, L. Zhang, A.L. Zhang, Activin b promotes bm-msc-mediated cutaneous wound healing by regulating cell migration via the jnk-erk signaling pathway, Cell Transplant. 23 (2014) 1061–1073.
[2] B.C. Heng, H. Liu, T. Cao, Transplanted human embryonic stem cells as biological 'catalysts' for tissue repair and regeneration, Med. Hypotheses 64 (2005) 1085–1088.
[3] C.M. Shi, T.M. Cheng, Y.P. Su, Y. Mai, J.F. Qu, X.Z. Ran, Transplantation of dermal multipotent cells promotes the hematopoietic recovery in sublethally irradiated rats, J. Radiat. Res. 45 (2004) 19–24.
[4] T.Y. Kim, D.S. Han, C.S. Eun, Y.W. Chung, Recombinant human epidermal growth factor enhances wound healing of pyoderma gangrenosum in a patient with ulcerative colitis, Inflamm. Bowel Dis. 14 (2008) 725–727.
[5] M.W. Tsang, W.K. Wong, C.S. Hung, K.M. Lai, W. Tang, E.Y. Cheung, G. Kam, L. Leung, C.W. Chan, C.M. Chu, E.K. Lam, Human epidermal growth factor enhances healing of diabetic foot ulcers, Diabetes Care 26 (2003) 1856–1861.
[6] D.L. Steed, Modifying the wound healing response with exogenous growth factors, Clin. Plast. Surg. 25 (1998) 397–405.

[7] K.D. Lee, T.K. Kuo, J. Whang-Peng, Y.F. Chung, C.T. Lin, S.H. Chou, J.R. Chen, Y.P. Chen, O.K. Lee, In vitro hepatic differentiation of human mesenchymal stem cells, Hepatology 40 (2004) 1275–1284.
[8] D. Orlic, J. Kajstura, S. Chimenti, D.M. Bodine, A. Leri, P. Anversa, Bone marrow stem cells regenerate infarcted myocardium, Pediatr. Transplant. 7 (2003) 86–88.
[9] S. Fukada, Y. Miyagoe-Suzuki, H. Tsukihara, K. Yuasa, S. Higuchi, S. Ono, K. Tsujikawa, S. Takeda, H. Yamamoto, Muscle regeneration by reconstitution with bone marrow or fetal liver cells from green fluorescent protein-gene transgenic mice, J. Cell Sci. 115 (2002) 1285–1293.
[10] D. Orlic, J. Kajstura, S. Chimenti, I. Jakoniuk, S.M. Anderson, B. Li, J. Pickel, R. McKay, B. Nadal-Ginard, D.M. Bodine, A. Leri, P. Anversa, Bone marrow cells regenerate infarcted myocardium, Nature 410 (2001) 701–705.
[11] G. Ferrari, G. Cusella-De Angelis, M. Coletta, E. Paolucci, A. Stornaiuolo, G. Cossu, F. Mavilio, Muscle regeneration by bone marrow-derived myogenic progenitors, Science 279 (1998) 1528–1530.
[12] L. Macri, R.A. Clark, Tissue engineering for cutaneous wounds: selecting the proper time and space for growth factors, cells and the extracellular matrix, Skin Pharmacol. Physiol. 22 (2009) 83–93.
[13] S.G. Priya, H. Jungvid, A. Kumar, Skin tissue engineering for tissue repair and regeneration, Tissue Eng. B Rev. 14 (2008) 105–118.
[14] J.A. Garlick, Engineering skin to study human disease–tissue models for cancer biology and wound repair, Adv. Biochem. Eng. Biotechnol. 103 (2007) 207–239.
[15] V. Dini, M. Romanelli, A. Piaggesi, A. Stefani, F. Mosca, Cutaneous tissue engineering and lower extremity wounds (part 2), Int. J. Lower Extremity Wounds 5 (2006) 27–34.
[16] S.P. Miguel, M.P. Ribeiro, H. Brancal, P. Coutinho, I.J. Correia, Thermoresponsive chitosan-agarose hydrogel for skin regeneration, Carbohydr. Polym. 111 (2014) 366–373.
[17] S.G. Choi, E.J. Baek, E. Davaa, Y.C. Nho, Y.M. Lim, J.S. Park, H.J. Gwon, K.M. Huh, J.S. Park, Topical treatment of the buccal mucosa and wounded skin in rats with a triamcinolone acetonide-loaded hydrogel prepared using an electron beam, Int. J. Pharm. 447 (2013) 102–108.
[18] S. Heilmann, S. Kuchler, C. Wischke, A. Lendlein, C. Stein, M. Schafer-Korting, A thermosensitive morphine-containing hydrogel for the treatment of large-scale skin wounds, Int. J. Pharm. 444 (2013) 96–102.
[19] M. Kedzierski, D. Lejman, D. Larysz, Hydrogel dressings in the treatment of wounds with skin defect complications, Ortopedia Traumatologia Rehabilitacja 3 (2001) 100–102.
[20] H.E. Bodde, E.A. Van Aalten, H.E. Junginger, Hydrogel patches for transdermal drug delivery; in-vivo water exchange and skin compatibility, J. Pharm. Pharmacol. 41 (1989) 152–155.
[21] H.Y. Lin, C.W. Peng, W.W. Wu, Fibrous hydrogel scaffolds with cells embedded in the fibers as a potential tissue scaffold for skin repair, Mater. Med. 25 (2014) 259–269.
[22] P. Paquet, C. Pierard-Franchimont, G.E. Pierard, P. Quatresooz, Skin fungal biocontamination and the skin hydrogel pad test, Arch. Dermatol. Res. 300 (2008) 167–171.
[23] X. Wang, S. Liu, Q. Zhao, N. Li, H. Zhang, X. Zhang, X. Lei, H. Zhao, Z. Deng, J. Qiao, Y. Cao, L. Ning, S. Liu, E. Duan, Three-dimensional hydrogel scaffolds facilitate in vitro self-renewal of human skin-derived precursors, Acta Biomater. 10 (2014) 3177–3187.
[24] C. Yang, L. Xu, Y. Zhou, X. Zhang, X. Huang, M. Wang, Y. Han, M. Zhai, S. Wei, J. Li, A green fabrication approach of gelatin/cm-chitosan hybrid hydrogel for wound healing, Carbohydr. Polym. 82 (2010) 1297–1305.
[25] Q.X. Ji, J. Deng, X.M. Xing, C.Q. Yuan, X.B. Yu, Q.C. Xu, J. Yue, Biocompatibility of a chitosan-based injectable thermosensitive hydrogel and its effects on dog periodontal tissue regeneration, Carbohydr. Polym. 82 (2010) 1153–1160.
[26] C. Weng, H. Dong, G. Chen, Y. Zhai, R. Bai, H. Hu, L. Lu, Z. Xu, Mir-409-3p inhibits ht1080 cell proliferation, vascularization and metastasis by targeting angiogenin, Cancer Lett. 323 (2012) 171–179.
[27] K. McFarlin, X. Gao, Y.B. Liu, D.S. Dulchavsky, D. Kwon, A.S. Arbab, M. Bansal, Y. Li, M. Chopp, S.A. Dulchavsky, S.C. Gautam, Bone marrow-derived mesenchymal stromal cells accelerate wound healing in the rat, Wound Repair Regen. 14 (2006) 471–478.
[28] M.W. Betz, P.C. Modi, J.F. Caccamese, D.P. Coletti, J.J. Sauk, J.P. Fisher, Cyclic acetal hydrogel system for bone marrow stromal cell encapsulation and osteodifferentiation, J. Biomed. Mater. Res. A 86 (2008) 662–670.
[29] M. Zhang, N.Y. Liu, X.E. Wang, Y.H. Chen, Q.L. Li, K.R. Lu, L. Sun, Q. Jia, L. Zhang, L. Zhang, Activin b promotes epithelial wound healing in vivo through rhoa-jnk signaling pathway, PLoS One 6 (2011) e25143.
[30] K.L. Kroeze, L. Vink, E.M. de Boer, R.J. Scheper, C. van Montfrans, S. Gibbs, Simple wound exudate collection method identifies bioactive cytokines and chemokines in (arterio) venous ulcers, Wound Repair Regen. 20 (2012) 294–303.
[31] S. Chen, J. Shi, M. Zhang, Y. Chen, X. Wang, L. Zhang, Z. Tian, Y. Yan, Q. Li, W. Zhong, Mesenchymal stem cell-laden anti-inflammatory hydrogel enhances diabetic wound healing, Sci. Rep. (2015), http://dx.doi.org/10.1038/srep18104.
[32] S. Chen, J. Shi, X. Xu, J. Ding, W. Zhong, L. Zhang, M. Xing, L. Zhang, Study of stiffness effects of poly (amidoamine)–poly (n-isopropyl acrylamide) hydrogel on wound healing, Colloids Surf. B: Biointerfaces 140 (2016) 574–582.
[33] J. Shi, J. Ouyang, Q. Li, L. Wang, J. Wu, W. Zhong, M.M.Q. Xing, Cell-compatible hydrogels based on a multifunctional crosslinker with tunable stiffness for tissue engineering, J. Mater. Chem. 22 (2012) 23952–23962.
[34] S. Chen, M. Zhang, X. Shao, X. Wang, L. Zhang, P. Xu, W. Zhong, L. Zhang, M. Xing, L. Zhang, A laminin mimetic peptide sikvav-conjugated chitosan hydrogel promoting wound healing by enhancing angiogenesis, re-epithelialization and collagen deposition, J. Mater. Chem. B 3 (2015) 6798–6804.
[35] B. Li, J.H.C. Wang, Fibroblasts and myofibroblasts in wound healing: force generation and measurement, J. Tissue Viability 20 (2011) 108.
[36] M. Zhang, N.-Y. Liu, X.-E. Wang, Y.-H. Chen, Q.-L. Li, K.-R. Lu, L. Sun, Q. Jia, L. Zhang, L. Zhang, Activin b promotes epithelial wound healing in vivo through rhoa-jnk signaling pathway, PLoS One 6 (2011) e25143.
[37] A. Pozzi, K.K. Wary, F.G. Giancotti, H.A. Gardner, Integrin α1β1 mediates a unique collagen-dependent proliferation pathway in vivo, J. Cell Biol. 142 (1998) 587–594.
[38] G.S. Schultz, G. Ladwig, A. Wysocki, Extracellular matrix: review of its roles in acute and chronic wounds, World Wide Wounds 2005 (2005).
[39] K.A. Bielefeld, S. Amini-Nik, B.A. Alman, Cutaneous wound healing: recruiting developmental pathways for regeneration, Cell. Mol. Life Sci. 70 (2013) 2059–2081.
[40] V.L. Martins, M. Caley, E.A. O'Toole, Matrix metalloproteinases and epidermal wound repair, Cell Tissue Res. 351 (2013) 255–268.
[41] A.J. Garber, M.J. Abrahamson, J.I. Barzilay, L. Blonde, Z.T. Bloomgarden, M.A. Bush, S. Dagogo-Jack, M.B. Davidson, D. Einhorn, W.T. Garvey, G. Grunberger, Y. Handelsman, I.B. Hirsch, P.S. Jellinger, J.B. McGill, J.I. Mechanick, P.D. Rosenblit, G.E. Umpierrez, M.H. Davidson, American association of clinical endocrinologists' comprehensive diabetes management algorithm 2013 consensus statement–executive summary, Endocr. Pract. 19 (2013) 536–557.
[42] A.J. Singer, R.A. Clark, Cutaneous wound healing, N. Engl. J. Med. 341 (1999) 738–746.
[43] J.J. Tomasek, J. McRae, G.K. Owens, C.J. Haaksma, Regulation of α-smooth muscle actin expression in granulation tissue myofibroblasts is dependent on the intronic carg element and the transforming growth factor-β1 control element, Am. J. Pathol. 166 (2005) 1343–1351.
[44] H.X. Shi, C. Lin, B.B. Lin, Z.G. Wang, H.Y. Zhang, F.Z. Wu, Y. Cheng, L.J. Xiang, D.J. Guo, X. Luo, G.Y. Zhang, X.B. Fu, S. Bellusci, X.K. Li, J. Xiao, The anti-scar effects of basic fibroblast growth factor on the wound repair in vitro and in vivo, PLoS One 8 (2013) e59966.
[45] J.L. Xie, H.N. Bian, S.H. Qi, H.D. Chen, H.D. Li, Y.B. Xu, T.Z. Li, X.S. Liu, H.Z. Liang, B.R. Xin, Y. Huan, Basic fibroblast growth factor (bfgf) alleviates the scar of the rabbit ear model in wound healing, Wound Repair Regen. 16 (2008) 576–581.